Optimal resolutions for IR spectroscopy through the OH Airglow

Paul Martini and D. L. DePoy

Department of Astronomy, Ohio State University,
140 W. 18th Avenue, Columbus, OH 43210, USA

ABSTRACT

The OH airglow emission lines are the dominant source of background emission in the near-infrared J and H bandpasses. In principle, these emission lines can be avoided by observing at sufficiently high spectral resolution, rejecting pixels contaminated by OH lines, and rebinning to the desired resolution. Two trade-offs to this approach are non-negligible detector noise per pixel and the added expense of instrumentation with higher resolution. In this contribution, we simulate various observed and desired resolutions as a function of detector noise and target brightness to develop a set of guidelines for the optimal resolution in a variety of observing programs. As a general rule, observing at a 2−pixel resolution of $2000 - 4000$ provides optimal OH rejection for a wide range of detector noise and source signal.

Keywords: near-infrared, spectroscopy, OH Airglow, OH Suppression

1. INTRODUCTION

Atmospheric OH airglow emission is the dominant source of background noise in ground-based astronomical observations from approximately 0.8μm $- 2.2\mu$m. For near-infrared observations, particularly through the atmospheric transmission windows that correspond to the J ($1.16 - 1.34\mu$m) and H ($1.5 - 1.8\mu$m) filter bandpasses, the OH airglow can contribute 92 – 98% and 98% of the background emission, respectively.[1,2] Removing this component could thus reduce the sky surface brightness from $\Sigma_J = 15.6$ and $\Sigma_H = 13.8$ mag arcsec^{-2} to below 18 mag arcsec^{-2} for both bands.[2] The reduction or elimination of this noise will result in a significant improvement in sensitivity to faint objects.

Many recent designs for near-infrared instrumentation on large telescopes have included hardware solutions to reduce or eliminate the OH airglow[3,4] (a process commonly referred to as OH Suppression). For near-infrared imaging, numerical calculations have shown that combinations of narrowband filters designed to avoid various combinations of OH airglow lines do not lead to improvements over broadband filters in H and provide only a marginal improvement in J.[2,5,6] This is because the OH airglow lines are relatively evenly distributed over these bands in lines of comparable brightness. Spectroscopy offers a more effective way to remove the OH airglow and several spectrographs, which mask out these emission lines, have been built.[7,8,3] These instruments reflect the dispersed input light off of a mirror, which is nonreflective at the wavelengths corresponding to the OH airglow lines.

In this contribution we present an alternate, software-only, approach to OH Suppression as an aid to both instrument designers and observers working in the near-infrared. We explore the option of observing at sufficient resolution to isolate the OH-contaminated regions to some fraction of the total observed spectrum while maximizing the signal-to-noise ratio (SNR). With modern, 2048x2048 pixel infrared arrays, it is possible to observe the entire J passband at a resolution as high as $R_J = 7100$ and the entire H passband at $R_H = 5600$. For low-resolution spectroscopy, we also explore the option of observing at sufficiently high resolution to avoid the OH airglow in some fraction of the bandpass and then rebin this spectrum to the target lower resolution. We discuss the details of these computations in the following section, including the various metrics we define to evaluate an optimal observing mode. In §3 we discuss our results and their dependence on observing conditions and instrument parameters.

Further author information: (Send correspondence to P.M.)
P.M.: E-mail: martini@astronomy.ohio-state.edu
D.L.D.: E-mail: depoy@astronomy.ohio-state.edu

2. SIGNAL-TO-NOISE RATIO CALCULATIONS

2.1. Overview

The wavelengths and intensities of the OH airglow lines have been measured by a number of investigators[9,10,1] and compiled by K. Ennico*. The intrinsic widths of these lines are extremely narrow; they are unresolved in observations with resolutions as high as $R \sim 100{,}000$. The lines also vary in intensity over the course of the night, both individually and as a whole. Generally, the lines vary over periods from tens of minutes to hours. The average intensity also decreases over the course of the night.[10]

For a noise-free detector, the optimal observing strategy is to obtain a spectrum with the highest resolution possible, reject the pixels containing an OH airglow line, and rebin the spectrum to the desired resolution to maximize the SNR. The non-negligible detector noise per pixel and the expense of constructing a high-resolution instrument make this approach impractical. Instead, there is a tradeoff between OH line rejection and larger effective detector noise as the resolution is increased. The purpose of this contribution is to calculate the optimal resolution that balances these two competing effects and will thus serve as a guideline for both near-infrared spectrograph design and observations with existing instrumentation.

2.2. Method

To assess the impact of the OH airglow on a near-infrared spectrum we need to numerically calculate the SNR on a pixel by pixel basis. The standard expression for the SNR is

$$SNR = \frac{N_S}{[N_S + N_B + N_D + N_R^2]^{1/2}}, \tag{1}$$

where N_S, N_B, N_D, and N_R are the signal in electrons due to the source, background, detector, and read noise, respectively. These quantities are

$$N_S = f_{\mathrm{OBJ}}\, t_{int}\, A_T\, \Delta\lambda\, \eta \tag{2}$$

$$N_B = f_{\mathrm{BKG}}\, t_{int}\, A_T\, \Delta\lambda\, \mathrm{d}\Omega\, \eta \tag{3}$$

$$N_D = D\, t_{int} \tag{4}$$

and the variables are defined in Table 1.

Table 1. Signal-to-Noise Ratio Parameters

Parameter	Name	Value	Units
f_{OBJ}	Object flux	see text	γ s^{-1} m^{-2} μm^{-1}
t_{int}	Integration time	600	s
A_T	Primary mirror aperture	8.4	m
η	System throughput	0.5	electrons γ^{-1}
f_{BKG}	Background flux	590	γ s^{-1} m^{-2} μm^{-1} arcsec^{-2}
dΩ	Slit area	0.08	arcsec^2
D	Dark current	0.05	electrons s^{-1}
N_R	Read Noise	5	electrons

These parameters are based on observations with a large telescope and sufficiently good seeing to justify a plate scale of $0.2''$ pixel^{-1}. Typical near-infrared spectroscopic observations are carried out with a maximum integration of on order 60 seconds due to the variations in the OH line intensities.[10] However, if these pixels are excluded,

*http://www.ast.cam.ac.uk/~optics/cohsi/www/ohsky/index.html

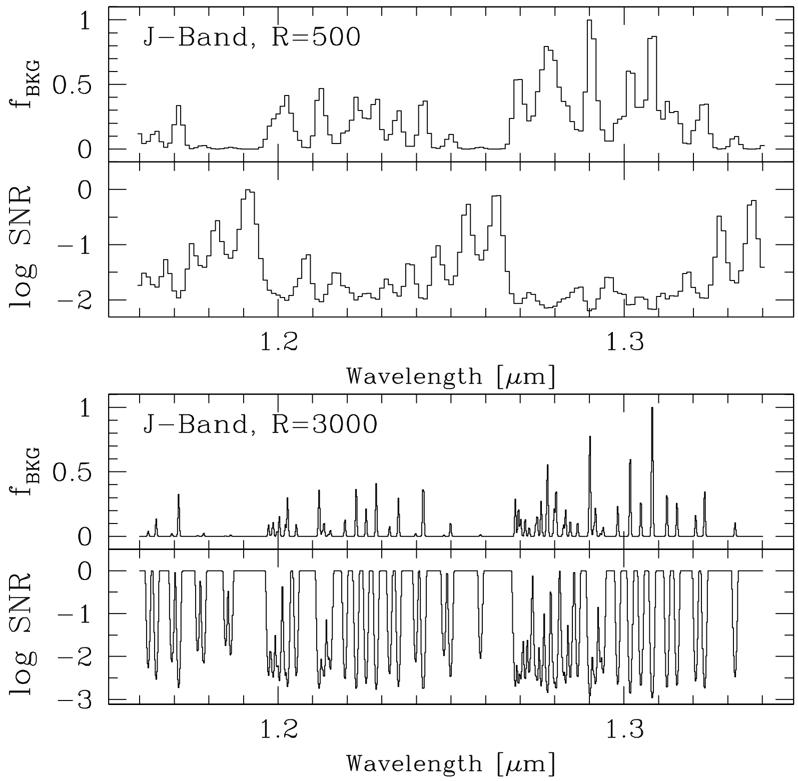

Figure 1. Relative background and SNR in the near-infrared $J-$band at a resolution of $R = 500$ (*upper 2 panels*). The background is normalized to the brightest OH airglow line. The SNR is normalized to the maximum SNR possible in the absence of the OH airglow. At $R = 500$ only one pixel is completely free of OH contamination. At $R = 3000$ (*lower 2 panels*) a large fraction of the spectrum is uncontaminated by the OH airglow.

significantly longer exposures should be possible, particularly if the saturation of the OH lines does not affect the neighboring pixels on the detector array. In the absence of OH airglow the limiting factor may be (currently unmeasured) variations in the continuum between the OH airglow lines, particularly for extended sources. The strength of this emission, hereafter referred to as the sky continuum, has been measured to be 590 γ s^{-1} m^{-2} μm^{-1} arcsec^{-2} at 1.665 μm on a dark night.[1] This emission was measured to be a factor of 15 higher on a bright night close to the nearly full moon, though the latter observations could be explained by an unusually large amount of scattering due to the presence of dust in the atmosphere from the eruption of Mt. Pinatubo. Other investigators[7,6] have used a sky continuum of 300 γ s^{-1} m^{-2} μm^{-1} arcsec^{-2} for J and 1200 γ s^{-1} m^{-2} μm^{-1} arcsec^{-2} for H. We discuss the impact of varying the sky continuum on our results in §3.3.

Another potentially significant source of background is scattering of dispersed OH airglow within the instrument itself. As mentioned above, the OH airglow contributes up to 98% of the total background. This implies that if even 2% is scattered out of the OH lines within the instrument, this instrumental background will be comparable to the sky continuum and could become the limiting factor in setting the overall performance. For the last two parameters in Table 1 we assumed a dark current typical of a HgCdTe device operating at the temperature of liquid N_2 and a somewhat low readnoise, though one which is obtainable with multiple samplings during the observation.[11]

In Figures 1 & 2 we show the background spectrum and corresponding SNR per pixel for a flat continuum source at J and H at a resolution of $R = 0.5\,\lambda_c/\Delta\lambda = 500$ (*upper two panels*) and 3000 (*lower two panels*). At $R = 500$ essentially none of the pixels are completely free of contamination by the OH airglow and this emission dominates the background noise. By $R = 3000$, however, nearly half of the pixels are completely free of OH airglow. The noise

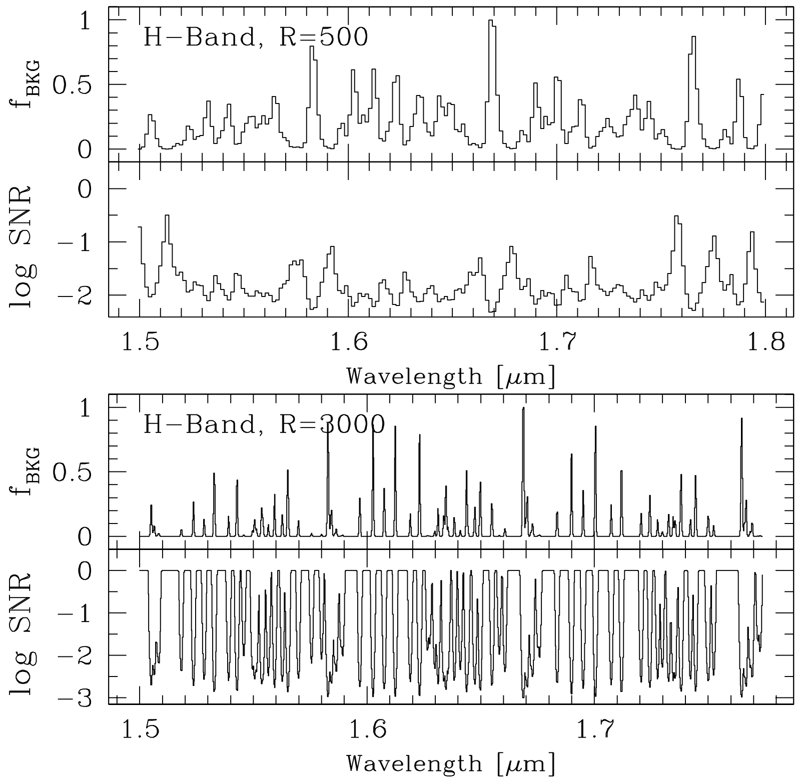

Figure 2. Same as Figure 1 for the near-infrared H−band.

in these pixels is instead set by the significantly lower sky continuum and detector noise. In these spectra and in all of our models we assume the instrumental profile of the OH airglow is Gaussian with full width at half maximum (FWHM) $= 2\,\Delta\lambda$, where $\Delta\lambda$ is set by the resolution.

2.3. Figures of Merit

The optimal resolution for observing a faint continuum source through the OH airglow lines will depend on the instrument parameters and the scientific goals of the project. This evaluation requires some metric or figure of merit to characterize the best resolution. One way is to consider the fraction of the bandpass that is completely free of OH airglow as a function of resolution. A graph of the "OH-free" fraction of the bandpass, as a function of resolution, is shown in Figure 3 for J (*upper panel*) and H (*lower panel*). The vertical, dashed lines in the figure mark the resolutions where 10%, 25%, and 50% of the bandpass is free of OH airglow.

The resolutions corresponding to the SNR in the best 10%, 25%, and 50% of the bandpass are useful figures of merit for evaluating the optimal resolution as a function of object brightness, sky continuum brightness, and detector noise. These different metrics could have application to a wide variety of observing programs. For example, if the goal of an observing program is to measure the slope of a target's continuum, it may suffice to only detect the continuum over 10% of the bandpass. However, if the goal is to fit the continuum to model spectral energy distributions, one may need to detect the continuum over a larger fraction of the bandpass. We calculate these figures of merit by rank-ordering the values for the SNR per pixel at a fixed resolution and selecting the SNR corresponding to the 10-, 25-, and 50-percentile value, which correspond to fixed fractions of the bandpass.

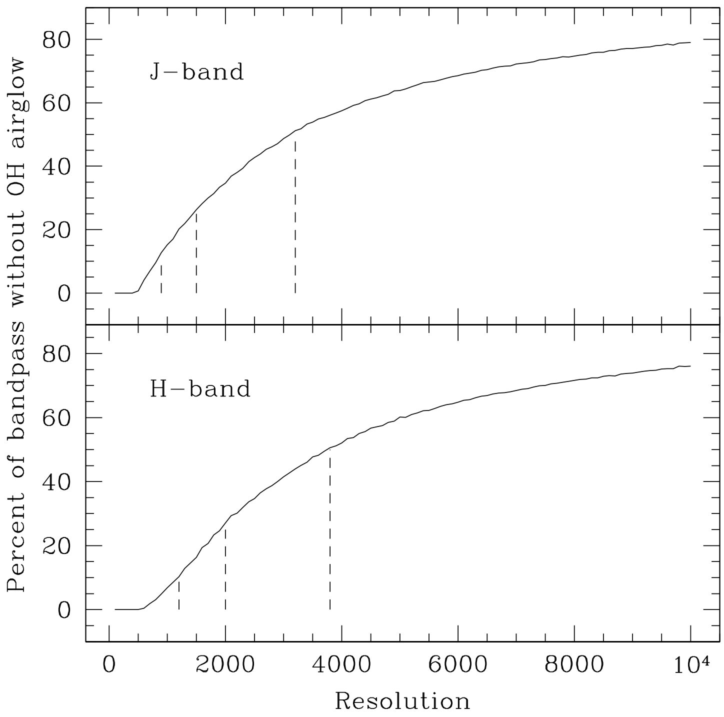

Figure 3. Fraction of pixels in the near-infrared J (*upper panel*) and H (*lower panel*) bandpasses free of OH contamination as a function of resolution. The vertical, dashed lines mark the resolutions where 10%, 25%, and 50% of the pixels are free of OH airglow. These lines correspond to R_J = 900, 1500, and 3200, respectively for J and R_H = 1200, 2000, and 3800 for H.

3. RESULTS

3.1. Optimal Resolutions

In Figure 4 we plot the SNR of a 20 mag object for the top 10%, 25% and 50% of the bandpass as a function of resolution for J (*upper panel*) and H (*lower panel*). This figure shows that if one only needs to detect the continuum in 10% of the bandpass, a resolution of $R_J \sim 900$ or $R_H \sim 1300$ would be the most efficient. To achieve a target SNR threshold over 50% of the bandpass, however, one should observe at a resolution of $R_J \sim 3200$ or $R_H \sim 3800$. The calculations presented in this section are based on the configuration listed in Table 1 and a J or $H = 20$ mag source with constant flux per unit wavelength.

3.2. Rebinning

Many astronomical observations only require the detection of the continuum of an object at low resolution. The best strategy with this criterion is to observe at sufficiently high resolution to observe between the OH lines and then rebin the uncontaminated pixels to improve the SNR. While Figures 1 and 2 clearly show that the background at a low resolution such as $R = 500$ is dominated by the OH airglow, one could also obtain an $R = 500$ spectrum by observing at a higher resolution, masking out the OH lines, and rebinning the spectrum to $R = 500$. To illustrate this approach, we adopted a target resolution of $R = 500$. We simulated observations from $R = 1000$ to 10,000 in steps of $\Delta R = 500$ and rebinned each spectrum to $R = 500$ after rejecting pixels severely contaminated by the OH airglow. To calculated the rebinned SNR, we rank-ordered the pixels in each bin by background noise. We then added pixels with progressively larger backgrounds until either all of the pixels were included in the bin or the addition of the next pixel decreased the SNR in the rebinned pixel. For apparent magnitudes from $15 - 25$, the optimal resolution for measuring 10% and 25% of the bandpass is $R_J = 1500$ and 2500, respectively, and $R_H = 2000$ and 3500. For 50%

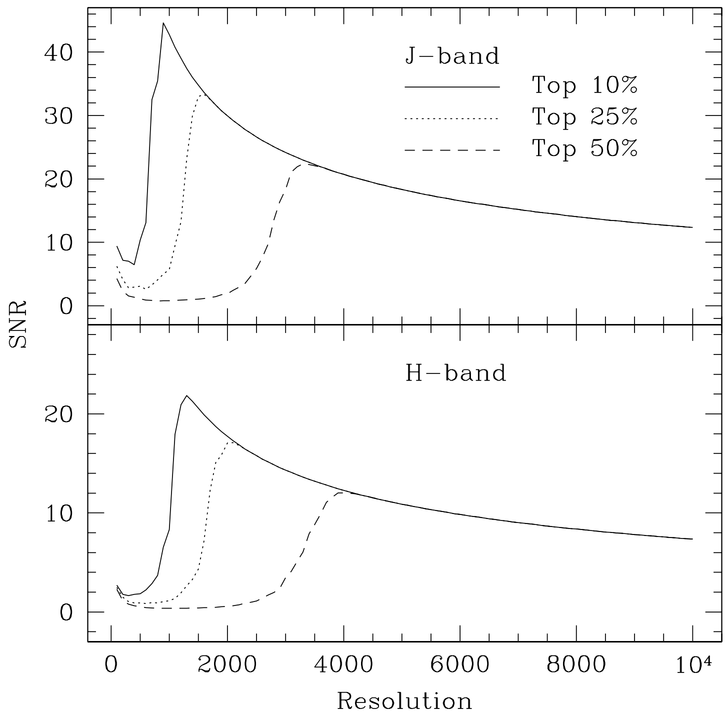

Figure 4. SNR corresponding to the top 10%, 25%, and 50% of the bandpass as a function of resolution for a flat continuum source with an apparent magnitude of J = 20 mag (*upper panel*) and H = 20 mag (*lower panel*). The peak SNR for the 10%, 25%, and 50% limits for J are at resolutions where 10%, 25%, and 50% of the pixels are completely free of OH emission, as marked by the vertical, dashed lines in Figure 3.

of the bandpass, $R = 4000$ provides a reasonable choice, though the SNR increases incrementally up to R =10,000. This is a reflection of the relatively even spacing of the OH lines within the J and H bandpasses.

3.3. Model Dependence

The SNR of an observation at a fixed spectroscopic resolution depends on the brightness of the object, the strength of the sky continuum, and noise from the detector. Ideally, the background noise (eq. [2.2]) will be solely determined by the sky continuum. However, any instrumental background not due to the detector itself (e.g., scattered light) will add to the sky continuum to determine the total background flux $f_{\rm BKG}$. The background noise also depends on the product of $f_{\rm BKG}$ and the area of the slit dΩ. An increase in dΩ therefore degrades the SNR by the same amount as a comparable increase in $f_{\rm BKG}$, assuming all of the light from the source passes through the slit. To test the robustness of our model, we have evaluated the figures of merit discussed in §2.3 as a function of object brightness for a range of values for the sky continuum and detector noise. The optimal resolutions for these different figures of merit change by less than ΔR = 200 when we vary the sky continuum or detector noise by a factor of four. Our results are relatively insensitive to these two sources of noise because the OH airglow is significantly stronger than the target's continuum. If OH airglow is present in a pixel it will always significantly degrade the SNR of this pixel regardless of the sky continuum or detector noise. The optimal resolution for faint objects is thus set by the fraction of pixels that are completely free of OH airglow. Another factor that could impact on our results is the instrumental profile. As stated in §2.2, we have assumed the OH lines are Gaussian. If the instrumental profile has broader wings, a larger fraction of the OH emission would spill into the neighboring pixels compared to the Gaussian case, at fixed resolution.

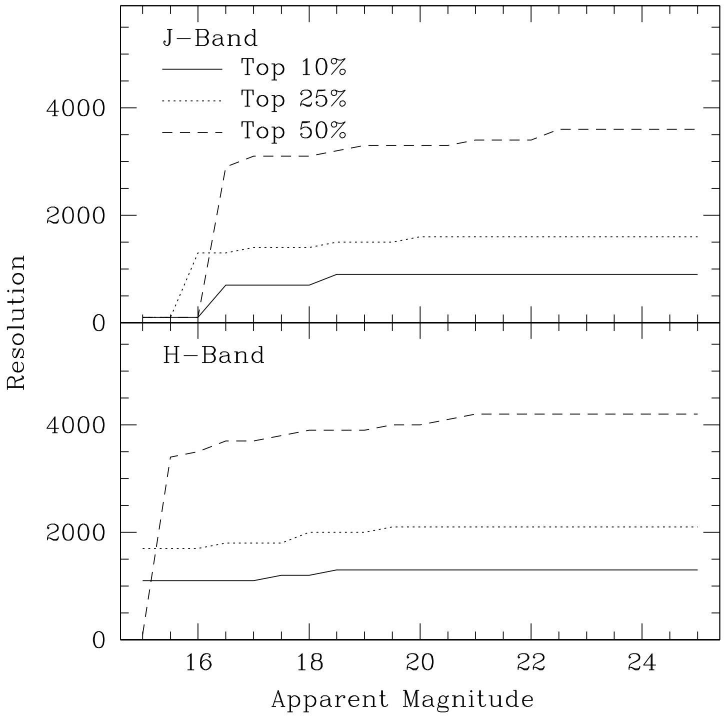

Figure 5. Optimal resolution to maximize the SNR in the top 10%, 25%, and 50% of the bandpass as a function of apparent magnitude in J (*upper panel*) and H (*lower panel*). At the brightest apparent magnitudes, a very low resolution is best as the object's brightness is comparable to the intensity of the OH airglow. For fainter J apparent magnitudes, the optimal resolution converges to $R_J = 900$, 1600, and 3600 for the maximum SNR in 10%, 25%, and 50% of the bandpass. The corresponding optimal resolutions for H are $R_H = 1300$, 2100, and 4200, respectively.

4. SUMMARY

The optimal resolution for observing through the OH airglow in the near-infrared J and H bands is an important quantity for instrument designers and observers. Due to the increasing cost of instrumentation with higher resolution, the optimal resolution for observing through the OH airglow can be an important factor in determining the capabilities of planned near-infrared spectrographs. Similarly, observers can benefit from this work by maximizing the SNR in their targets and thus attain the greatest possible scientific return from their observing run.

We have found that resolutions of $R = 2000 - 4000$ maximize the SNR in observations of a continuum source over a wide range of object brightness. This result is relatively independent of the sky continuum brightness and detector noise, though clearly minimizing detector noise and scattered light within the instrument can still have a significant impact on the SNR. If the detection of faint continuum sources, from faint stars to high-redshift galaxies, is the primary science driver for a near-infrared spectrograph, then resolutions above $R = 4000$, and their associated greater expense and lower SNR per pixel, are unnecessary.

ACKNOWLEDGMENTS

We would like to thank Rick Pogge and Andy Stephens for helpful comments on the manuscript. This work was supported in part by a PEGS grant to the Department of Astronomy at The Ohio State University.

REFERENCES

1. T. Maihara, F. Iwamuro, T. Yamashita, D. N. B. Hall, L. L. Cowie, A. T. Tokunaga, and A. Pickles, "Observations of the OH airglow emission," *Pub. Astro. Soc. Pac.* **105**, pp. 940–944, 1993.

2. T. M. Herbst, "Numerical evaluation of OH-suppression instruments," *Pub. Astro. Soc. Pac.* **106**, pp. 1298–1309, 1994.
3. K. A. Ennico, I. R. Parry, M. A. Kenworthy, R. S. Ellis, C. D. Mackay, M. G. Beckett, A. Aragón-Salamanca, K. Glazebrook, J. Brinchmann, J. Pritchard, S. Medlen, F. Piché, R. McMahon, and F. Cortecchia, "The Cambridge OH Suppression Instrument (COHSI): Status after first commissioning run," in *Infrared Astronomical Instrumentation*, A. M. Fowler, ed., *Proc. SPIE* **3354**, pp. 668–674, 1998.
4. K. Motohara, T. Maihara, F. Iwamuro, S. Oya, M. Imanishi, H. Terada, M. Goto, J. Iwai, H. Tanabe, H. Tsukamoto, and K. Sekiguchi, "CISCO: A Cooled Infrared Spectrograph and Camera for OHS," in *Infrared Astronomical Instrumentation*, A. M. Fowler, ed., *Proc. SPIE* **3354**, pp. 659–665, 1998.
5. R. Content, "Deep-sky infrared imaging by reduction of the background light. I. sources of the background and potential suppression of the OH emission," *Astrophys. Journal* **464**, pp. 412–425, 1996.
6. D. H. Jones, J. Bland-Hawthorn, and M. G. Burton, "Numerical evaluation of OH airglow suppression filters," *Pub. Astro. Soc. Pac.* **108**, pp. 929–938, 1996.
7. F. Iwamuro, T. Maihara, S. Oya, H. Tsukamoto, D. N. B. Hall, L. L. Cowie, A. T. Tokunaga, and A. J. Pickles, "Development of an OH-airglow suppressor spectrograph," *Publ. Astron. Soc. Japan* **46**, pp. 515–521, 1994.
8. F. Piché, I. Parry, K. Ennico, R. Ellis, J. Pritchard, C. Mackay, and R. McMahon, "COHSI: The Cambridge OH Suppression Instrument," in *Optical Telescopes of Today and Tomorrow*, A. L. Ardeberg, ed., *Proc. SPIE* **2871**, pp. 1332–1341, 1997.
9. E. Oliva and L. Origlia, "The OH airglow spectrum: a calibration source for infrared spectrometers," *Astron. Astrophys.* **254**, pp. 466–471, 1992.
10. S. K. Ramsay, C. M. Mountain, and T. R. Geballe, "Non-thermal emission in the atmosphere above Mauna Kea," *Mon. Not. Roy. Astro. Soc.* **259**, pp. 751–760, 1992.
11. A. Fowler and I. Gatley, "Demonstration of an algorithm for read-noise reduction in infrared arrays," *Astrophys. Journal* **353**, pp. L33–L34, 1990.